# Dominant factors controlling the efficiency of two-phase flow cleaning in spiral-wound membrane elements

Y. Wibisono[a,b,d], F. Ahmad[a], E.R. Cornelissen[c], A.J.B. Kemperman[a,*], K. Nijmeijer[a]

[a]Faculty of Science and Technology, Membrane Science and Technology, MESA + Institute of Nanotechnology, University of Twente, P.O. Box 217, 7500 AE Enschede, The Netherlands, Tel. +31 53 4892956; Fax: +31 53 4894611;
emails: a.j.b.kemperman@utwente.nl (A.J.B. Kemperman), y_wibisono@ub.ac.id (Y. Wibisono)
[b]Wetsus, Centre of Excellence for Sustainable Water Technology, P.O. Box 1113, 8900 CC Leeuwarden, The Netherlands
[c]KWR Watercycle Research Institute, P.O. Box 1072, 3430 BB Nieuwegein, The Netherlands
[d]Faculty of Agricultural Technology, Division of Bioprocess Engineering, Department of Agricultural Engineering, University of Brawijaya, Malang 65145, Indonesia

**ABSTRACT**

Two-phase flow cleaning has been successfully applied to control fouling in spiral wound membrane elements. This study focuses on its experimental optimization using a Taguchi Design of Experiment method (L-25 orthogonal arrays) to elucidate the influence of different factors and to reveal the important one(s) affecting the cleaning efficiency of two-phase flow cleaning. All possible combinations of the factors, i.e. feed type, spacer geometry, gas/liquid ratio, and liquid velocity, each at five levels were evaluated. The main effect of each factor on the efficiency of two-phase flow cleaning was measured by determining the performance response (mean of cleaning efficiency) and by calculating the mean signal-to-noise ratio. An analysis of variance was applied to calculate the relative contribution of each factor on the efficiency of two-phase flow cleaning. The results showed that the feed type is by far the most essential factor contributing to the cleaning efficiency. The spacer geometry is ranked second, followed by the gas/liquid ratio and the liquid velocity, which both have an only very minor effect on the cleaning performance. In terms of practical application, the operator should consider first the type of foulant prior to taking a decision on whether or not two-phase flow cleaning will be effective. Once the foulant type is defined, the use of the highest gas/liquid ratio, the highest liquid velocity, and the thickest feed spacer (diamond type) are recommended to achieve maximum two-phase flow cleaning efficiency.

*Keywords:* Two-phase flow; Membrane fouling; Membrane cleaning; Taguchi method; Spiral wound membrane

## 1. Introduction

About 80% of the world's inhabitants do not have access to clean water for drinking and sanitation [1], although technological investments on modern water treatment systems via the use of alternative water sources such as saline water and recycling used water, has increased significantly the reliability of future supply [2]. Conventional treatment processes, e.g. coagulation–flocculation–sedimentation,

*Corresponding author.

adsorption, and chlorination, fail to get rid of all contaminants in potable water sources and triggered the development of advanced water treatment approaches such as the use of membranes [3]. Membrane technology is now being used widely for purification of water and wastewater, providing superiority in terms of a small foot print, short construction times, cost-effectiveness, clean, easy, and long-term reliable operation while producing high rejection rates for contaminants [4]. Nanofiltration (NF) and low pressure reverse osmosis (RO) membranes are among the most efficient to treat water for drinking purposes, due to an adequate rejection of divalent and multivalent ions (water softening) combined with a lower rejection of monovalent ions such as sodium chloride (low changes in water salinity). Moreover, NF and low pressure RO have an increased rejection of dissolved organic as well as emerging contaminants and produce high water fluxes at a relatively low feed pressure [5]. Yet, a major shortcoming of the application of membranes in water and wastewater treatment is membrane fouling. Membrane fouling in NF/RO systems employing spiral wound membrane modules, e.g. biofouling, causes a feed channel pressure drop (FCP) increase and permeate flux decline, leading to extensive expenses on pumping energies and cleaning chemicals.

Two-phase flow cleaning can effectively remove biofouling in spiral wound membrane elements often used in NF/RO systems, and hence enhance membrane process performance [6,7]. In a preliminary study [8], we have shown that feed spacer geometry, gas/liquid ratio, liquid velocity, and foulant type, all turned out to affect the two-phase flow cleaning efficiency. The spacer geometry determined the channel porosity and channel hydraulic diameter, and hence influenced the two-phase flow cleaning efficiency. The gas/liquid ratio was crucial to generate a good bubble distribution with full channel coverage by the bubbles. The liquid superficial velocity affected the bubble velocity, and thus is an important parameter to improve the two-phase flow cleaning efficiency. Moreover, we concluded from the study that a colloidal type of fouling was easier to remove from spacer-filled membrane channels compared to macromolecular fouling, i.e. fouling by organic foulants, yet it is expected that is depends on the interaction energy of the foulants. In a following work [9], we have reported that two-phase flow cleaning was able to mitigate biofouling in spacer-filled membrane channels.

Despite these observations, a systematic study, investigating the specific contribution and importance of each of these parameters on the efficacy of two-phase

flow cleaning in spiral wound membrane elements is missing still. Understanding of the dominant factors and mutual interactions between the different factors in this case is essential to further improve the effect of two-phase flow on the process performance of NF and RO membrane processes for drinking water production and wastewater treatment. In order to obtain a systematic understanding of the effect of the relevant factors in two-phase flow cleaning, we investigated the influence of foulant type, spacer geometry, gas/liquid ratio, and liquid velocity, each at five different levels on the efficiency of two-phase flow cleaning applied in spacer-filled membrane channels. The Taguchi method, a developed optimization method to analyze experimental results and find possible correlations, is employed. We study and report the importance of the different factors on their ability to promote high efficiency two-phase flow cleaning.

## 2. Experimental

### 2.1. Materials

Five different foulant compositions were selected, serving as representative model foulant. Sodium alginate (SA) and humic acid (HA) were selected as model organic foulants. Alginate and HA have been identified as major organic components in natural water and they have been extensively used to study membrane fouling in pressure-driven membrane processes [10]. Both SA (Sigma-Aldrich) and HA (Acros Organics) were received in powder form and used as received. Fresh solutions of SA and HA were prepared prior to each experiment by dispersing 1 g of SA or HA powder, respectively, in 1 L of deionized water with a conductivity of less than 1 µS/cm (Milli-Q, Millipore, USA), under constant magnetic stirring for at least 2 h until no more sedimentation occurred [11]. To increase the particle adhesion to the membrane surface, 4 or 10 mM calcium chloride (Sigma-Aldrich) was added to the solutions [12].

Dry yeast (Dr Oetker, Bielefeld, Germany) was selected as model foulant for colloidal particle fouling. Although normally wastewater contains iron or silica colloidal particles, since their activity (solubility and mobility) is very dependent on the water pH, it is very difficult to use these particles as model foulants. The ferric state (Fe(III)) of iron particles is insoluble in water at neutral pH, and the ferrous state (Fe(II)) could easily be changed to Fe(III) by aerating the water at a neutral pH [13–16]. For silica particles, activity under various pH conditions was described in ASTM D4993-89, also indicating pH dependency. Yeast colloidal particle is less sensitive to pH changes,

and therefore was chosen by us as a model for colloidal fouling.

An untreated yeast suspension was prepared by mixing 3 g of dry yeast into 0.3 L of deionized water and then stirring for half an hour to complete dissolution. Yeast washing was conducted according to a procedure described by Ye and Chen [17] and Çulfaz et al. [18], as follows: the unwashed yeast was centrifuged at a speed of 2,500 rpm for 10 min. The suspension liquid was then drawn out using a syringe and discharged, while the yeast sediment was collected by a lab spoon. The above process was repeated twice. Washed yeast was then dried under airflow for 24 h. After the washing process, the weight ratio of dry washed yeast to dry unwashed yeast was found to be 70%. All yeast concentrations in our experiments were concentrations based on dry washed yeast. Yeast solutions were prepared by dissolving 1 g of washed and dried yeast in 1 L of deionized water (Milli-Q, Millipore, USA), under constant magnetic stirring until complete dissolution. Particle size and distribution of all solutions containing alginates, HAs, or yeast were determined using a Zetasizer Nano ZS and Mastersizer 2000 (Malvern).

To create biofouling, tap water was enriched with nutrients. The nutrients added were sodium acetate ($CH_3COONa$) to provide C, sodium nitrate ($NaNO_3$) for N, and anhydrous monobasic sodium phosphate ($NaH_2PO_4$) for P addition, respectively. Nutrients were added at a molar ratio of C:N:P = 100:20:10 to enhance biofouling growth. All nutrients were purchased from Sigma-Aldrich and used as received [9,19].

Commercially available thin-film composite polyamide NF membrane sheets (Hydranautics ESNA1-LF2-LD, Oceanside, California, USA) were used. The same membranes were used in all our previous studies [9,19]. The ESNA1 is a low pressure NF membrane and is widely applied in water reclamation applications. The membranes were extensively rinsed with and soaked in Milli-Q water before use.

Five different spacers were selected, all commonly used in practice in spiral wound membrane modules. The five spacers differed in terms of thickness and filament angle. The filament angle is the angle between two crossing spacer filaments facing the channel axis [8]. An overview of the spacer geometries is presented in Table 1. The pictures of the different spacers and corresponding spacer code are shown in Fig. 1.

## 2.2. Liquid velocity and gas/liquid ratio

The foulant type and feed spacer geometry as described above are categorized as discrete factors. Discrete factors are defined as factors which only have discrete values, one state or another. The liquid velocity and gas/liquid ratio on the other hand are

Table 1
Selected spacer geometries used in this study

| Channel gap ($10^3$ m) | Spacer geometries | | | | |
| | Average thickness ($10^{-3}$ m) | Shape | Filament angle (°) | Supplier | Spacer code |
| --- | --- | --- | --- | --- | --- |
| 0.5 | 0.508[a] | Diamond | 90 | Naltex | A |
| | 0.508[a] | Diamond | 60 | Naltex | B |
| 0.7 | 0.800[b] | Diamond | 90 | Trisep | C |
| | 0.650[b] | Diamond | 90 | Hydranautics | D |
| 1.2 | 1.2[b] | Diamond | 90 | Toray | E |

[a]Manufacturers' data.
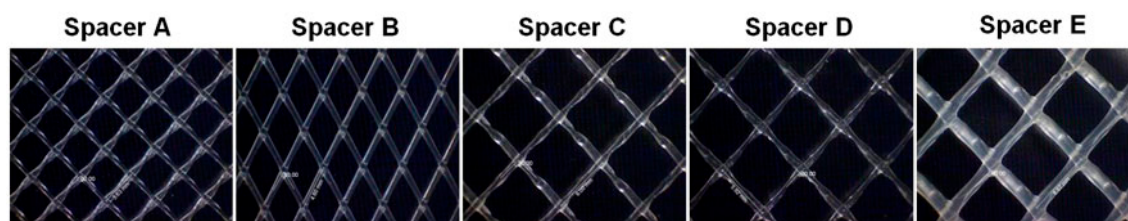[b]Measured using a digital caliper.



Fig. 1. Images of investigated feed spacers.

categorized as continuous factors, as these can be adjusted in a continuous manner over a wide range of values to carry out the experiments [20]. Cross-flow velocities selected in our experiments are common for lead elements in industrial installations [21], i.e. a constant liquid velocity ($u_L$) of 0.04, 0.06, 0.07, 0.082, and 0.116 m/s. Moreover, the gas/liquid ratio is an important factor affecting the recovery of the FCP and the flux [6]. The gas/liquid ratio ($\theta$) used during two-phase flow cleaning is defined as:

$$\theta \equiv \frac{u_G}{u_G + u_L} \tag{1}$$

where $u_G$ and $u_L$ are the superficial velocities of the gas and the liquid (m/s), respectively. The gas/liquid ratio ranged from 0.167, 0.33, 0.412, 0.5, and 0.629, associated with bubble and slug flow patterns in two-phase flow [6]. The gas flow set by the mass flow controller is defined at 0°C and 1 atm; the ideal gas law was used to correct for this and obtain the actual gas flow.

### 2.3. Experimental factors and levels

Table 2 summarizes the experimental factors and their corresponding levels as selected for this study.

### 2.4. Operational protocol

All measurements were characterized by their FCP ($\Delta P$). The FCP is a simple but sensitive parameter that corresponds to the resistance in the feed flow channel and is not affected by the flux [22].

Each experiment consisted of two stages: (1) a *fouling stage*, in which the fouling on the membrane and spacer was allowed to develop until a certain FCP increase over the feed channel was reached (approximately 100% FCP increase for colloidal fouling (HA, SA, yeast) and 300% FCP increase for biofouling, relative to its initial value) and (2) *a cleaning stage*, in which gas/liquid two-phase flow was introduced to the fouled cells. Once the FCP of the flow cell had increased until a certain level as set before (100% or 300% FCP increase), the fouling stage was considered complete and the cleaning stage was started. The cleaning stage was conducted for 60 s for all experiments. After completion of the two-phase flow cleaning, the operating conditions were restored to those of the fouling stage and the FCP of the cleaned flow cell was measured again. Exact details of the experimental conditions, set-ups, and flow cell simulators used for both colloidal/organics fouling and biofouling experiments are described elsewhere [8,9].

The performance of two-phase flow cleaning was evaluated in terms of cleaning efficiency ($\eta$), which is defined as:

$$\eta = \frac{(\Delta P_t - \Delta P_{TPF})}{(\Delta P_t - \Delta P_0)} \times 100\% \tag{2}$$

where $\Delta P_0$ is the initial FCP (mbar), $\Delta P_t$ is the FCP at time $t$ (100% FCP increase for colloidal fouling and 300% FCP increase for biofouling, relative to $\Delta P_0$) when two-phase flow cleaning was performed (mbar). $\Delta P_{TPF}$ is the FCP after two-phase flow cleaning (mbar).

### 2.5. Taguchi method

The modern methods of design and analysis of experiments involving multiple factors (parameters or variables) and replicated trials were first developed by Fisher [23]. Fisher called his method for the systematic

Table 2
Experimental factors and corresponding five levels studied

| Factors | Levels | | | | |
| | 1 | 2 | 3 | 4 | 5 |
| --- | --- | --- | --- | --- | --- |
| Feed type | Tap water + 1,000 µg C/L (C:N:P 100:20:10) | Humic acid 1,000 ppm + 4 mM CaCl$_2$ | Sodium alginate 1,000 ppm + 4 mM CaCl$_2$ | Humic acid 1,000 ppm + 10 mM CaCl$_2$ | Washed yeast, 1,000 ppm |
| Liquid velocity (m/s) | 0.04 | 0.06 | 0.07 | 0.082 | 0.116 |
| Gas/liquid ratio (–) | 0.167 | 0.33 | 0.412 | 0.5 | 0.629 |
| Spacer geometry | A | B | C | D | E |

and efficient investigation on the relevance of a parameter on an output variable in a multiple parameter system "factorial design in experimentation", which later popularly became well known as "factorial design of experiments" [24]. A full factorial design includes all possible combinations of factors; hence it requires a large number of experiments when it involves a significant number of factors, such as is often the case in manufacturing industries. Taguchi proposed a versatile approach on the design of experiments that allowed the selection of the smallest set of experiments from all possibilities, still providing sufficient information on the effect of a certain parameter and cross effects of different parameters. Hence, the Taguchi approach reduces the number of experiments significantly without excluding the influence of all factors, nor neglecting consistency and reproducibility [25]. The Taguchi method provides a shortcut to design experiments based on a set of orthogonal arrays (OAs) [26]. A comprehensive explanation of this design of experiments approach using the Taguchi method can be found elsewhere [20].

As we have four controllable factors (feed type, liquid velocity, gas/liquid ratio, and spacer geometry) with five different levels each (see Table 2), an L-25 OA for the Taguchi method and design of experiments was selected. In a conventional full factorial design, this would require a total number of $5^4 = 625$ experimental trials to study four controllable factors each at five levels. Using the Taguchi method, only 25 experiments are necessary, hence this decreases drastically the experimental time, while, when performed systematically, still provides the necessary information. Each experiment was repeated twice under the same conditions to investigate noise effects with respect to two-phase flow cleaning efficiency. Noise factors are those factors that do influence the response but cannot be controlled in the actual application, such as humidity, ambient temperature, or operators [25]. To take into account these noise factors and to avoid any influence of the experimental set-up on the output data, the experiments were conducted randomly (not in sequence) at different times. Table 3 summarizes the L-25 OAs of the 25 experimental trials and the

Table 3
Structure of the Taguchi L-25 OA scheme [27]

| Experiment trial | Factors and their levels[a] | | | |
| | Feed type | Liquid velocity (m/s) | Gas/liquid ratio (–) | Spacer geometry |
|---|---|---|---|---|
| 1 | 1 | 1 | 1 | 1 |
| 2 | 1 | 2 | 2 | 2 |
| 3 | 1 | 3 | 3 | 3 |
| 4 | 1 | 4 | 4 | 4 |
| 5 | 1 | 5 | 5 | 5 |
| 6 | 2 | 1 | 2 | 3 |
| 7 | 2 | 2 | 3 | 4 |
| 8 | 2 | 3 | 4 | 5 |
| 9 | 2 | 4 | 5 | 1 |
| 10 | 2 | 5 | 1 | 2 |
| 11 | 3 | 1 | 3 | 5 |
| 12 | 3 | 2 | 4 | 1 |
| 13 | 3 | 3 | 5 | 2 |
| 14 | 3 | 4 | 1 | 3 |
| 15 | 3 | 5 | 2 | 4 |
| 16 | 4 | 1 | 4 | 2 |
| 17 | 4 | 2 | 5 | 3 |
| 18 | 4 | 3 | 1 | 4 |
| 19 | 4 | 4 | 2 | 5 |
| 20 | 4 | 5 | 3 | 1 |
| 21 | 5 | 1 | 5 | 4 |
| 22 | 5 | 2 | 1 | 5 |
| 23 | 5 | 3 | 2 | 1 |
| 24 | 5 | 4 | 3 | 2 |
| 25 | 5 | 5 | 4 | 3 |

[a]Actual values for Levels 1–5 used in the tests can be found in Table 2.

combination of the different factors and their corresponding levels.

The main effect of each controllable factor was defined as the performance response (PR), which is the mean of the cleaning efficiency of each duplicate ($\eta_1$ and $\eta_2$). The corresponding signal-to-noise ($S/N$) ratio is defined as the ratio of the power of a signal (response) to the power of the noise (error). We choose "the higher, the better" to define how the factors contribute to the efficiency of two-phase flow cleaning. The $S/N$ ratio (SNR) of this "the higher, the better" approach [20] is then defined as:

$$\text{SNR} = -10 \log \left[ \frac{1}{n} \left( \sum_{i=1}^{n} \frac{1}{y_i^2} \right) \right] \qquad (3)$$

where $n$ is the number of trials ($n = 2$ in this study) and $y_i$ is the observed PR (in this study).

Since the Taguchi method replaces a full factorial set of experiments by a leaner and faster partial factorial set of experiments, the confidence interval of the results is based on the variance. For this purpose, an analysis of variance (ANOVA) was used. Comparison of the different variances subsequently allows determining the relative contribution of each of the different factors. The ANOVA was conducted using Design-Expert v6.0 software (Stat-Ease Inc., Minneapolis, MN, USA), which calculates the degree of freedom, the sum of square, the variance (mean squares), the experimental error, the totals of the results, and the percentage contribution of each controllable factor.

## 3. Results and discussion

### 3.1. Particle size and particle size distribution

Fig. 2 shows the particle size and particle size distribution of the different foulants used in this study: freshly prepared HA, SA, unwashed, and washed yeast (all at a concentration of 1 g/L, without salt).

After washing, the average particle size of the yeast particles shifted from approximately 3.80 μm to slightly smaller sizes (approx. 2.88 μm). The yeast particles are the biggest particles used. The HA particles are 0.55 μm and the alginate particle size is 0.068 μm. Prior to the experiments, $CaCl_2$ was added to the HA and SA solutions to enhance the fouling tendency of the colloids. The $Ca^{2+}$ ions added enhance the interaction between the HA or SA molecules [11], resulting in an increased fouling tendency. A higher fouling rate is desirable, as the objective of this study is to define the dominant factor(s) determining the
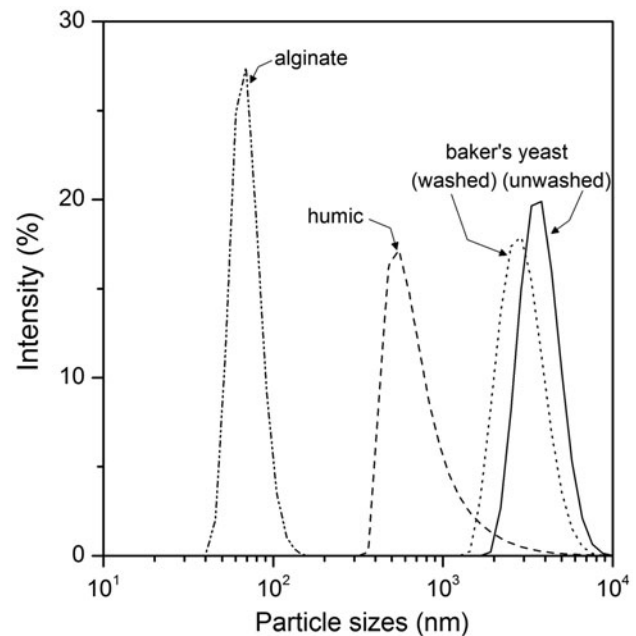


Fig. 2. Particle sizes and particle-size distributions of colloid particles (without salt added) used as feed suspensions as determined by dynamic light scattering at 25°C.

efficiency of the two-phase flow cleaning process. Hence, the investigation focuses on the cleaning stages and not on the fouling stage in itself. Shorter fouling stages shorten the duration of the experiments. It is worth mentioning that two-phase flow cleaning might be less efficient in real applications, compared to the cleaning efficiency obtained for this accelerated fouling study. This is due to the specific characteristics of the fouling layer formed. Accelerated fouling may result in film structures different than the ones obtained in natural fouling. Parameters like structure and compactness determine the specific effectiveness of two-phase flow cleaning in removing fouling. Nevertheless, the results obtained from this study in terms of dominant factors remain valid.

### 3.2. Pressure drop recovery

Fig. 3 shows the pressure drop recovery in terms of two-phase flow cleaning efficiency for all 25 experiments (in duplicate) as calculated using Eq. (2). The results of the duplicates are shown as a standard error.

As shown in Fig. 3, the two-phase flow cleaning efficiency varies between approximately 15 and 93%. As the error bars clearly show, the noise factors are not very significant and do not disturb the response, except for experiments 3, 6, 22, and 23. However, in
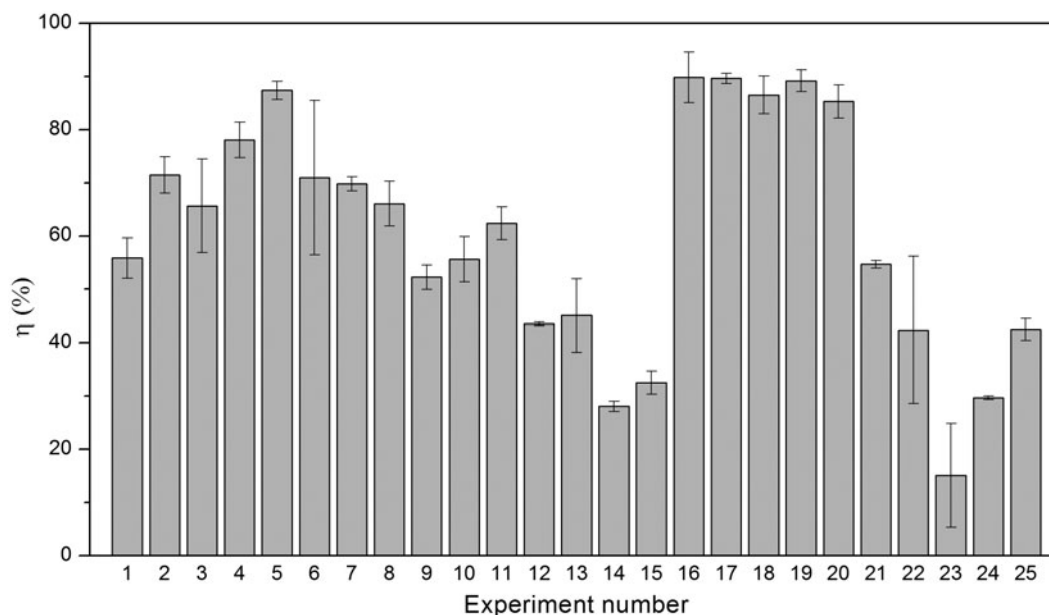
Fig. 3. Two-phase flow cleaning efficiency of each experiment (all experiments performed in duplicate, shown as error bars). Numbers on the X-axis correspond to the experiment number, as summarized in Table 3.

the Taguchi method, this deviation is included in the SNR analysis. When the trend is similar, the noise factor is not considered significant.

None of the results shows a total (100%) recovery of the pressure drop, meaning that some fouling remained in the feed channels for all combination of factors.

### 3.3. S/N ratio analysis

The Taguchi method using OAs is a powerful tool for analyzing the influence of controllable factors on the PR (i.e. average two-phase flow cleaning efficiency in this study). Table 4 summarizes the different set values and corresponding obtained experimental data for each experiment. In Table 4, each column represents the L-25 OA based on the standard OA as shown in Table 3. The very left column shows the experiment number, each number in a row represents a combination of factor levels. The next four columns are the controllable factors tested in this study: feed type, liquid velocity, gas/liquid ratio ($\theta$), and spacer geometry. The four columns on the right are the responses obtained from the experimental trials. $\eta_1$ is the two-phase flow cleaning efficiency of the experiment and $\eta_2$ is the duplicate of the same experiment. The PR is the mean value of the two running efficiencies ($\eta_1$ and $\eta_2$), and shows the nominal response of each experimental trials. The very right column is the SNR, calculated using Eq. (3). The SNR is calculated

from the PR value and represents the deviation of the response due to noise factors. In this work, noise factors include small variations in room temperature, humidity, uniformity of the feed solutions, interaction of foulants with membrane/feed spacer surfaces, and influence of operating conditions on the membranes.

Both the SNR and the maximum PR rely on the approach "the higher, the better". The "signal" in the SNR is the value of the desired output parameter (mean of $\eta$). The "noise" represents the value of the undesired output parameter (standard deviation). Therefore, the SNR is the ratio of the mean and the standard deviation. The use of highest SNR means a smaller variability. Since the experimental design is orthogonal, the effect of each factor at all different levels can be, for instance, the mean PR and SNR for the feed type at level 1, 2, 3, 4, and 5, and can be calculated by averaging the PR and SNR values in Table 4 for the experiments 1–5, 6–10, 11–15, 16–20, and 21–25, respectively. In a similar manner, the mean PR and SNR values for all other factors at all levels can be calculated as well. The main contribution of each controllable factor to the PR (in %) and the corresponding SNR values are shown in Fig. 4.

The strength of this approach and more specifically Fig. 4 is that it immediately shows the relevant variables that control and determine the performance. In terms of application, this means that Fig. 4 directly shows the possibilities an operator of a membrane water purification plant has on how and to what

Table 4
Selected values of controllable factors, corresponding calculated two-phase flow cleaning efficiency of the duplicate experiments ($\eta_1$ and $\eta_2$), PR value and SNR obtained for the 25 experiments carried out in this study

| Exp. trial | Feed type | Liquid velocity (m/s) | G/L ratio ($\theta$) | Spacer | $\eta_1$ | $\eta_2$ | PR | SNR |
|---|---|---|---|---|---|---|---|---|
| 1 | Tap water + C:N:P 100:20:10 | 0.04 | 0.167 | A | 53.15 | 58.54 | 55.85 | 34.9 |
| 2 | Tap water + C:N:P 100:20:10 | 0.06 | 0.33 | B | 73.86 | 69.07 | 71.47 | 37.1 |
| 3 | Tap water + C:N:P 100:20:10 | 0.07 | 0.412 | C | 71.87 | 59.44 | 65.66 | 36.3 |
| 4 | Tap water + C:N:P 100:20:10 | 0.082 | 0.5 | D | 75.72 | 80.41 | 78.07 | 37.8 |
| 5 | Tap water + C:N:P 100:20:10 | 0.116 | 0.629 | E | 88.59 | 86.13 | 87.36 | 38.8 |
| 6 | Humic acid 1,000 ppm + 4 mM $CaCl_2$ | 0.04 | 0.33 | C | 60.68 | 81.20 | 70.94 | 37.0 |
| 7 | Humic acid 1,000 ppm + 4 mM $CaCl_2$ | 0.06 | 0.412 | D | 70.75 | 68.84 | 69.80 | 36.9 |
| 8 | Humic acid 1,000 ppm + 4 mM $CaCl_2$ | 0.07 | 0.5 | E | 63.10 | 69.05 | 66.08 | 36.4 |
| 9 | Humic acid 1,000 ppm + 4 mM $CaCl_2$ | 0.082 | 0.629 | A | 50.64 | 53.89 | 52.27 | 34.4 |
| 10 | Humic acid 1,000 ppm + 4 mM $CaCl_2$ | 0.116 | 0.167 | B | 52.65 | 58.68 | 55.67 | 34.9 |
| 11 | Sodium alginate 1,000 ppm + 4 mM $CaCl_2$ | 0.04 | 0.412 | E | 60.22 | 64.56 | 62.39 | 35.9 |
| 12 | Sodium alginate 1,000 ppm + 4 mM $CaCl_2$ | 0.06 | 0.5 | A | 43.28 | 43.79 | 43.54 | 32.8 |
| 13 | Sodium alginate 1,000 ppm + 4 mM $CaCl_2$ | 0.07 | 0.629 | B | 40.25 | 49.95 | 45.10 | 33.1 |
| 14 | Sodium alginate 1,000 ppm + 4 mM $CaCl_2$ | 0.082 | 0.167 | C | 27.38 | 28.74 | 28.06 | 29.0 |
| 15 | Sodium alginate 1,000 ppm + 4 mM $CaCl_2$ | 0.116 | 0.33 | D | 34.08 | 31.00 | 32.54 | 30.2 |
| 16 | Humic acid 1,000 ppm + 10 mM $CaCl_2$ | 0.04 | 0.5 | B | 93.18 | 86.44 | 89.81 | 39.1 |
| 17 | Humic acid 1,000 ppm + 10 mM $CaCl_2$ | 0.06 | 0.629 | C | 88.95 | 90.29 | 89.62 | 39.0 |
| 18 | Humic acid 1,000 ppm + 10 mM $CaCl_2$ | 0.07 | 0.167 | D | 84.00 | 89.00 | 86.50 | 38.7 |
| 19 | Humic acid 1,000 ppm + 10 mM $CaCl_2$ | 0.082 | 0.33 | E | 90.59 | 87.74 | 89.17 | 39.0 |
| 20 | Humic acid 1,000 ppm + 10 mM $CaCl_2$ | 0.116 | 0.412 | A | 87.49 | 83.08 | 85.29 | 38.6 |
| 21 | Yeast 1,000 ppm | 0.04 | 0.629 | D | 55.16 | 54.19 | 54.68 | 34.8 |
| 22 | Yeast 1,000 ppm | 0.06 | 0.167 | E | 32.62 | 52.14 | 42.38 | 32.5 |
| 23 | Yeast 1,000 ppm | 0.07 | 0.33 | A | 8.19 | 22.01 | 15.10 | 23.6 |
| 24 | Yeast 1,000 ppm | 0.082 | 0.412 | B | 29.43 | 29.95 | 29.69 | 29.5 |
| 25 | Yeast 1,000 ppm | 0.116 | 0.5 | C | 41.05 | 43.93 | 42.49 | 32.6 |

extent to increase the cleaning efficiency of two-phase flow cleaning resulting in increased flux values. Fig. 4 shows that the PR and SNR values vary with all controllable factors and that in general the PR and SNR values show similar trends. However, the effect of the feed type (foulant) is by far the most dominant, compared to the other factors. So, in order to increase the efficiency of two-phase flow cleaning, the highest effect can be expected when the feed type and foulant is controlled. In practice, this means the choice for the suitable pre-treatment techniques are very important to enhance the process efficiency. Also, control of the other three factors (liquid velocity, gas/liquid ratio, and spacer type) does have an effect, but the response is less strong and the increase in efficiency is less.

Two-phase flow cleaning works effectively to remove fouling by HAs with added 10 mM $CaCl_2$. On the other hand, the cleaning efficiency is lowest for removing fouling caused by washed yeast and alginates. The two-phase flow cleaning efficiencies for HA + 4 mM $CaCl_2$ and biofouling are fairly better.

When $CaCl_2$ is added to HA solutions, $Ca^{2+}$ ions bind to the carboxylate and phenolate groups of the HAs and enhance the interaction between the HA molecules. The higher the $Ca^{2+}$ ion concentration, the stronger this molecular interaction; the calcium ions may promote the formation of aggregates or form a physical bridge between foulants and membrane surface [11]. These larger particles easily clog narrow, spacer-filled channels, decrease porosity, and therefore lead to a greater increase in the FCP, in case HA + 10 mM $CaCl_2$ solutions are used when compared to the use of a HA + 4 mM $CaCl_2$ feed solution. These bigger, clogged particles are at the same time more easy to remove by two-phase flow cleaning, hence the cleaning efficiency is higher for HA + 10 mM $CaCl_2$ solutions than for HA + 4 mM $CaCl_2$ feed solutions.

Fouling by organic macromolecules, including HAs and alginates, is developed by binding of the carboxylic functional groups. The presence of $Ca^{2+}$ ions facilitates a more complex binding and increases foulant-foulant intermolecular interactions. The adhesion forces of alginates are much stronger than those of HAs in the presence of $Ca^{2+}$ ions, and alginates form a cross-linked network by intermolecular bridging [28,29]. Also, the foulant-membrane surface intermolecular interactions are enhanced when $Ca^{2+}$ ions
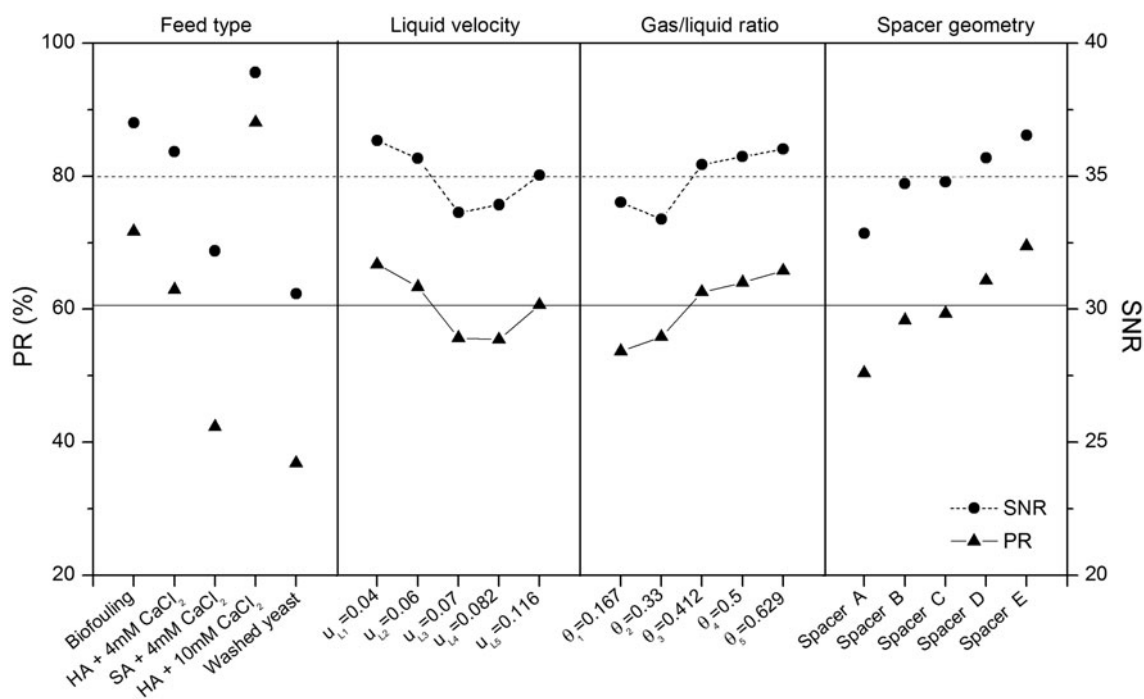
Fig. 4. Variation of cleaning efficiency and SNR for the controllable factors investigated. HA = humic acid, $u_L$ = liquid velocity (m/s) and $\theta$ = gas/liquid ratio. The two horizontal lines represent the mean PR and SNR of all controllable factors.

are present, inducing a strong interaction between the carboxylic groups of the organic macromolecular particles (HAs and alginates) and the functional groups on the membrane surface and the feed spacer [30]. Since the adhesion forces of alginates are much stronger than those of HAs [30], alginate binding to the membrane surface is also much stronger. Consequently, when a hydrodynamic force is applied to remove this fouling, as in two-phase flow cleaning, the effect of the bubbles on removal of alginate fouling is less than when removing HA fouling. In addition, the presence of divalent $Ca^{2+}$ ions also induce the formation of gel-like structures in the case of alginates [31] that are more difficult to remove by two-phase flow cleaning as well.

Regarding biofouling removal, as we found in our previous work [9], the use of a feed solution consisting of tap water with addition of a high concentration of nutrients (1 mg Ac-C/L) is able to accelerate biofilm growth in spacer-filled membrane channels. However, the use of this nutrient concentration produces a thick, but fluffy biofilm in the feed channel in relatively short times of only 5–7 d that can also be easily removed by two-phase flow cleaning, hence resulting in a relatively good biofilm removal of approximately 70%. The use of a lower amount of nutrients would

decrease the biofilm growth, and produce more dense biofouling layers. However, that would take too much experimental time for this study, while not adding essential information at this stage. Nevertheless, the obtained results can be considered as representative in terms of dominance of the different factors.

Due to their larger size, deposition of yeast particles is driven by random Brownian diffusion of yeast cells to the NF membrane surface [32]. At the earlier stages, individual cells deposit at different locations on membrane and feed spacer surfaces, followed by the deposition and adhesion of new yeast cells onto the already deposited cells and the formation of aggregates. These aggregates are "sticky" and two-phase flow cleaning to a large extent fails to remove all aggregates completely from the feed spacer channels.

Although a continuous factor, as shown in Fig. 4, the effect of the liquid velocity on the two-phase flow cleaning efficiency is less essential. The efficiency is highest when the liquid velocity is lowest ($u_L$ = 0.04 m/s), showing a minimum when $u_L$ = 0.07–0.082 m/s. Liquid velocities used were always equal in both the fouling and corresponding cleaning stage for each specific experiment. When the lowest liquid velocity is applied during the fouling stage, shear forces are low, and hence more

fouling can develop in the feed spacer channel. Consequently, a 100% FCP increase was obtained faster [8], and a thick but less compact fouling was formed. This thick fouling layer can be easily removed by two-phase flow cleaning, leading to the highest cleaning efficiency. At intermediate velocities ($u_L = 0.06$–$0.082$ m/s), the formed fouling layer is more compact. At these intermediate velocities, however, shear forces are not so dominant and two-phase flow cleaning is not so efficient yet, which is visible as a minimum in Fig. 4. At the highest liquid velocity ($u_L = 0.116$ m/s) investigated, however, a more dense fouling layer is formed during the fouling stage. Also during the cleaning stage, this high liquid velocity is applied. This significantly affects the gas bubble velocity as well (as shown in [8]) and creates additional and higher shear forces on the fouling layer, and hence the cleaning efficiency is increased again.

The effect of gas/liquid ratio is obvious, although less dominant than the foulant type. As found in many applications of two-phase flow cleaning processes, a higher gas/liquid ratio promotes higher cleaning efficiency [6]. A higher gas/liquid ratio introduces more bubbles, and consequently more shear and a better cleaning efficiency is obtained.

For the discrete variable spacer type, the efficiency increases going from spacer A to E. The highest cleaning efficiency is found when the thickest spacer (1.2 mm) is used. However, not only the spacer thickness is responsible for the higher cleaning efficiency, also e.g. the filament length as well as hydraulic diameter and the specific spacer surface chemistry and area play a role. As it is a discrete factor, a specific trend in terms of the individual and combined effects of these spacer characteristics cannot be distinguished at this stage. The results are in agreement with what we found in our previous work [8].

### 3.4. ANOVA analysis

In order to define the variance and significance of the contribution of each controllable factor, an ANOVA was performed on the experimental data. The results are summarized in Table 5.

Table 5 presents the degrees of freedom, the sum of squares, the variance (mean squares), the percentage contribution, and the process influence rank of each controllable factor on the output PR (i.e. two-phase flow cleaning efficiency). By definition, the degrees of freedom for a factor equals the number of levels for that specific factor minus 1 [25]. ANOVA reveals that the feed type contributes for more than 78% to the two-phase flow cleaning efficiency, while the contributions of all other factors are (far) less than 10%. The feed type therefore is the major, essential factor determining the efficiency. Flux enhancement and fouling removal efficiency increase can therefore best be reached by changing the feed (as far as that is possible in practical applications by applying a suitable pre-treatment), as this has by far the highest impact. As presented in Table 5, the spacer geometry is ranked second, followed by the gas/liquid ratio and the liquid velocity, which both have an only very minor effect. In terms of practical applications, however, especially these last two parameters are the easiest to change, as these are two operating parameters, while the other two factors are usually system characteristics that cannot be easily changed.

### 3.5. Applicability of process optimization

The Taguchi method and the subsequent calculation of the SNR and ANOVA for all combinations of controllable factors is a valuable, efficient tool to predict optimum conditions for a certain process, without running a full set of experiments changing each variable individually. At a later stage, a subsequent additional confirmation experiment can be conducted.

In this study, the objective was to determine the dominant factor determining the two-phase flow cleaning efficiency in spiral wound membrane elements. As half of the controllable factors tested here are discrete factors (feed type and spacer geometry), the results of the optimization analysis do not directly give precise insights into the specific improvements of

Table 5
ANOVA for the PR

| Controllable factors | Degrees of freedom | Sum of squares | Variance | Percent contribution | Process influencing rank |
|---|---|---|---|---|---|
| Feed type | 4 | 8,900.76 | 2,225.19 | 78.11 | 1 |
| Liquid velocity (m/s) | 4 | 478.27 | 119.57 | 4.20 | 4 |
| Gas/liquid ratio | 4 | 563.02 | 140.75 | 4.94 | 3 |
| Spacer geometry | 4 | 1,014.29 | 253.57 | 8.90 | 2 |
| Error | 8 | 438.16 | 54.77 | 3.85 | |
| Total | 24 | 11,394.5 | | 100 | |

these two factors regarding two-phase flow cleaning efficiency, but they do show the relevance of the different factors. Only continuous factors (in this case, the gas/liquid ratio and the liquid velocity) can be directly and easily optimized using this analysis.

More practically, in order to use the results of this study in practical applications of two-phase flow cleaning, the operator or engineer should consider first the type of foulant prior to taking a decision on whether or not to clean by two-phase flow. Once the feed type is defined, the use of the highest gas/liquid ratio, the highest liquid velocity, and the thickest feed spacer (diamond type) are recommended to achieve maximum two-phase flow cleaning efficiency. In order to achieve the highest liquid velocity and the highest gas/liquid ratio, the operator should increase pumping capacity for the liquid phase and gas compressor capacity for the gas phase. The energy consumption will be higher by applying those actions. However, the consumption will still be lower compared to the increase in pumping energy due to the fouling phenomena.

## 4. Conclusions

In this study, the dominant factor in terms of two-phase flow cleaning efficiency in spiral wound membrane elements was determined using a Taguchi design of experiment with a L-25 OA. Four controllable factors (feed type, feed spacer geometry, gas/liquid ratio, and liquid velocity) were tested at five different levels. Analysis of responses was conducted, and the SNR and an ANOVA were determined. This approach clearly revealed that the feed type is the most crucial factor determining the efficiency of two-phase flow cleaning. The spacer geometry is ranked second, followed by the gas/liquid ratio and the liquid velocity, which both have a very minor effect.

## Acknowledgments

## Nomenclature

| | | |
|---|---|---|
| ANOVA | — | analysis of variance |
| $\sigma$ | — | filament angle (°) |
| $\eta$ | — | two-phase flow cleaning efficiency (%) |
| $\Delta P_0$ | — | initial feed channel pressure drop (mbar) |
| $\Delta P_t$ | — | feed channel pressure drop in $t$-time (mbar) |
| $\Delta P_{TPF}$ | — | feed channel pressure drop post two-phase flow cleaning (mbar) |
| $\theta$ | — | gas/liquid ratio (–) |
| SNR | — | signal-to-noise ratio |
| OA | — | orthogonal array |
| $P_{gas}$ | — | gas pressure (bar) |
| $u_G$ | — | superficial gas velocity (m/s) |
| $u_L$ | — | superficial liquid velocity (m/s) |

## References

[1] C.J. Vörösmarty, P. McIntyre, M.O. Gessner, D. Dudgeon, A. Prusevich, P. Green, S. Glidden, S.E. Bunn, C.A. Sullivan, C.R. Liermann, Global threats to human water security and river biodiversity, Nature 467 (2010) 555–561.

[2] J.D. Brookes, C.C. Carey, D.P. Hamilton, L. Ho, L. van der Linden, R. Renner, A. Rigosi, Emerging challenges for the drinking water industry, Environ. Sci. Technol. 48 (2014) 2099–2101.

[3] V. Likodimos, D. Dionysiou, P. Falaras, Clean water: Water detoxification using innovative photocatalysts, Rev. Environ. Sci. Biotechnol. 9 (2010) 87–94.

[4] T. Peters, Membrane technology for water treatment, Chem. Eng. Technol. 33 (2010) 1233–1240.

[5] K.V. Plakas, A.J. Karabelas, Removal of pesticides from water by NF and RO membranes—A review, Desalination 287 (2012) 255–265.

[6] Y. Wibisono, E.R. Cornelissen, A.J.B. Kemperman, W.G.J. van der Meer, K. Nijmeijer, Two-phase flow in membrane processes: A technology with a future, J. Membr. Sci. 453 (2014) 566–602.

[7] E.R. Cornelissen, M.A. Pot, R.C.M. Jong, J.A. De Ruijter, E.F. Beerendonk, J.M.C. van Agtmaal, One year of experience with air/water cleaning in spiral wound RO membranes for surface water treatment. in: J. Pinnekamp, M. Wessling, T. Melin (Eds.), 6th IWA Specialist Conference on Membrane Technology for Water and Wastewater Treatment, International Water Association, Aachen, 2011, pp. 219–220.

[8] Y. Wibisono, Two-phase Flow for Fouling Control in Membranes, PhD thesis, University of Twente, 2014.

[9] Y. Wibisono, K.E. El Obied, E.R. Cornelissen, A.J.B. Kemperman, K. Nijmeijer, Biofouling removal in spiral-wound nanofiltration elements using two-phase flow cleaning, J. Membr. Sci. 475 (2015) 131–146.

[10] Q. She, Y.K.W. Wong, S. Zhao, C.Y. Tang, Organic fouling in pressure retarded osmosis: Experiments, mechanisms and implications, J. Membr. Sci. 428 (2013) 181–189.

[11] W.J.C. van de Ven, K.v.t. Sant, I.G.M. Pünt, A. Zwijnenburg, A.J.B. Kemperman, W.G.J. van der Meer, M. Wessling, Hollow fiber dead-end ultrafiltration: Influence of ionic environment on filtration of alginates, J. Membr. Sci. 308 (2008) 218–229.

[12] S. Lee, J. Cho, M. Elimelech, Influence of colloidal fouling and feed water recovery on salt rejection of RO and NF membranes, Desalination 160 (2004) 1–12.

[13] K. Kuma, J. Nishioka, K. Matsunaga, Controls on iron (III) hydroxide solubility in seawater: The influence of pH and natural organic chelators, Limnol. Oceanogr. 41 (1996) 396–407.

[14] K.H. Gayer, L. Woontner, The solubility of ferrous hydroxide and ferric hydroxide in acidic and basic media at 25°, J. Phys. Chem. 60 (1956) 1569–1571.

[15] S. Chaturvedi, P.N. Dave, Removal of iron for safe drinking water, Desalination 303 (2012) 1–11.

[16] Ş. İrdemez, N. Demircioğlu, Y.Ş. Yildiz, The effects of pH on phosphate removal from wastewater by electrocoagulation with iron plate electrodes, J. Hazard. Mater. 137 (2006) 1231–1235.

[17] Y. Ye, V. Chen, Reversibility of heterogeneous deposits formed from yeast and proteins during microfiltration, J. Membr. Sci. 265 (2005) 20–28.

[18] P.Z. Çulfaz, M. Haddad, M. Wessling, R.G.H. Lammertink, Fouling behavior of microstructured hollow fibers in cross-flow filtrations: Critical flux determination and direct visual observation of particle deposition, J. Membr. Sci. 372 (2011) 210–218.

[19] Y. Wibisono, W. Yandi, M. Golabi, R. Nugraha, E.R. Cornelissen, A.J.B. Kemperman, T. Ederth, K. Nijmeijer, Hydrogel-coated feed spacers in two-phase flow cleaning in spiral wound membrane elements: A novel platform for eco-friendly biofouling mitigation, Water Res. 71 (2015) 171–186.

[20] R.K. Roy, Design of Experiments Using The Taguchi Approach: 16 Steps to Product and Process Improvement, John Wiley & Sons Inc., New York, NY, 2001.

[21] J.S. Vrouwenvelder, C. Hinrichs, W.G.J. Van der Meer, M.C.M. Van Loosdrecht, J.C. Kruithof, Pressure drop increase by biofilm accumulation in spiral wound RO and NF membrane systems: role of substrate concentration, flow velocity, substrate load and flow direction, Biofouling 25 (2009) 543–555.

[22] J.S. Vrouwenvelder, C. Hinrichs, A.R. Sun, F. Royer, J.A.M. van Paassen, S.M. Bakker, W.G.J. van der Meer, J.C. Kruithof, M.C.M. van Loosdrecht, Monitoring and control of biofouling in nanofiltration and reverse osmosis membranes, Water Sci. Technol. Water Supply 8 (2008) 449–458.

[23] F. Yates, Sir Ronald Fisher and the design of experiments, Biometrics 20 (1964) 307–321.

[24] J.F. Box, R.A. Fisher and the design of experiments, 1922–1926, Am. Stat. 34 (1980) 1–7.

[25] R.K. Roy, A Primer on the Taguchi Method, Society of Manufacturing Engineers, Michigan, 1990.

[26] T.J. Robinson, C.M. Borror, R.H. Myers, Robust parameter design: A review, Qual. Reliab. Eng. Int. 20 (2004) 81–101.

[27] P. Saudagar, R. Singhal, A statistical approach using L25 orthogonal array method to study fermentative production of clavulanic acid by Streptomyces clavuligerus MTCC 1142, Appl. Biochem. Biotechnol. 136 (2007) 345–359.

[28] B. Mi, M. Elimelech, Chemical and physical aspects of organic fouling of forward osmosis membranes, J. Membr. Sci. 320 (2008) 292–302.

[29] S. Lee, M. Elimelech, Relating organic fouling of reverse osmosis membranes to intermolecular adhesion forces, Environ. Sci. Technol. 40 (2006) 980–987.

[30] Q. Li, M. Elimelech, Organic fouling and chemical cleaning of nanofiltration membranes: Measurements and mechanisms, Environ. Sci. Technol. 38 (2004) 4683–4693.

[31] A.J. de Kerchove, M. Elimelech, Formation of polysaccharide gel layers in the presence of $Ca^{2+}$ and $K^+$ ions: Measurements and mechanisms, Biomacromolecules 8 (2007) 113–121.

[32] A. Subramani, E.M.V. Hoek, Direct observation of initial microbial deposition onto reverse osmosis and nanofiltration membranes, J. Membr. Sci. 319 (2008) 111–125.